Spin fluctuations in the spin-Peierls compound MEM(TCNQ)$_2$ studied using muon spin relaxation

B. W. Lovett,* S. J. Blundell, F. L. Pratt,† Th. Jestädt, and W. Hayes
Clarendon Laboratory, University of Oxford, Parks Road, Oxford OX1 3PU, United Kingdom

S. Tagaki
Department of Physics, Kyushu Institute of Technology, Tobata, Kitakyushu 804, Japan

M. Kurmoo
IPCMS, 23 rue du Loess, BP 20/CR, 67037 Strasbourg Cedex, France
(Received 22 March 1999; revised manuscript received 3 November 1999)

We report a muon spin relaxation (μSR) investigation of the organic spin-Peierls compound MEM(TCNQ)$_2$ at temperatures down to 39 mK. We have observed a slowing down of the electronic spins as the spin-Peierls gap widens at temperatures below the spin-Peierls transition and use this behavior to estimate the size of the gap. At the very lowest temperatures the electronic spin fluctuations freeze out and the muon spin depolarization is dominated by a persistent static mechanism which we ascribe to a defect-spin system. We relate the low-temperature depolarization rate to the concentration of these defects, and we propose a model for the creation of spin defects by the muon itself.

I. INTRODUCTION

The spin-Peierls (SP) transition[1] is an intrinsic magnetoelastic instability which occurs in one-dimensional antiferromagnetic spin chains.[2,3] A coupling between the electronic spins and the three-dimensional lattice phonons results in a dimerized ground state below a transition temperature T_{SP}. Above this temperature, the chains may be characterized by a single antiferromagnetic exchange constant J acting between adjacent spins. Below T_{SP}, the dimerization results in two alternating, unequal exchange constants, $J_{1,2}=J[1\pm d(T)]$. This gives rise to a gap in the magnetic excitation spectrum, which separates a singlet, nonmagnetic ground state from a band of triplet magnon excitations.[4] The difference between the exchange constants increases as the dimerization becomes more pronounced; the magnetic gap reaches a maximum at $T=0$ and according to the Hartree-Fock theory of Pytte[4] follows a BCS-like relation, falling to zero at T_{SP}.

In this paper, we report a significant extension of our preliminary muon spin relaxation (μSR) study[5] of the organic SP compound methyl-ethyl-morpholinium (tetracyanoquinodimethanide)$_2$ [MEM(TCNQ)$_2$], whose molecular structure is shown in Fig. 1. This charge-transfer complex consists of one-dimensional stacks of planar TCNQ molecules, each of which has a charge of $-\frac{1}{2}e$ associated with it. Adjacent stacks are separated by arrangements of MEM$^+$ cations. It undergoes two structural transformations. The first, which occurs at 335 K, is a conventional Peierls (P) transition[6] in which the uniform TCNQ chains dimerize.[7] This results in a change from metallic to insulating behavior as a single electronic charge becomes localized on each TCNQ dimer; the single spin on each dimer couples antiferromagnetically to its neighbors. This phase persists down to the SP transition at 18 K, where a dimerization of the TCNQ dimers takes place (this is a tetramerization of the original chain).[8,9]

Evidence from studies of the far-infrared spectrum of MEM(TCNQ)$_2$ (Refs. 10 and 11) indicates that the SP transition is driven by a coupling to a low-energy phonon mode along the TCNQ stack which softens below T_{SP}. This is not surprising in this organic compound where weak van der Waals forces are primarily responsible for the molecular bonding. Electron-spin-resonance,[12,13] nuclear-magnetic-resonance,[14] and magnetic susceptibility[7] measurements confirm the low-temperature magnetic transition to a split-off singlet ground state in MEM(TCNQ)$_2$.

Pytte's treatment[4] may be used to relate the transition temperatures to the relevant coupling constants; whereas the conventional Peierls distortion is expected at a temperature $T_P \sim (E_F/k_B)\exp(-1/\alpha_{e\text{-}ph})$, where E_F is the Fermi energy of the system and $\alpha_{e\text{-}ph}$ is the electron-phonon coupling constant, the spin-Peierls transition is expected at $T_{SP} \sim (J/k_B)\exp(-1/\alpha_{s\text{-}ph})$, where $\alpha_{s\text{-}ph}$ is the spin-phonon coupling constant. $J \ll E_F$ and hence $T_{SP} \ll T_P$.[3] (More elaborate theories[15] give a slightly different dependence, though the proportionality of T_{SP} and J is general.)

II. EXPERIMENTAL METHOD

Our sample of MEM(TCNQ)$_2$ was prepared in Kyushu (Japan) and the SP transition was identified by carrying out a

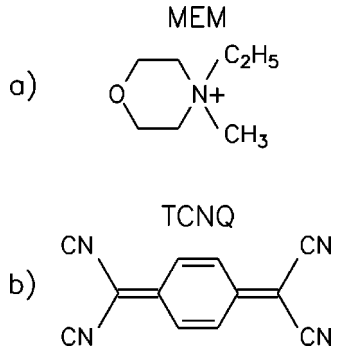

FIG. 1. Molecular structure of (a) MEM and (b) TCNQ.

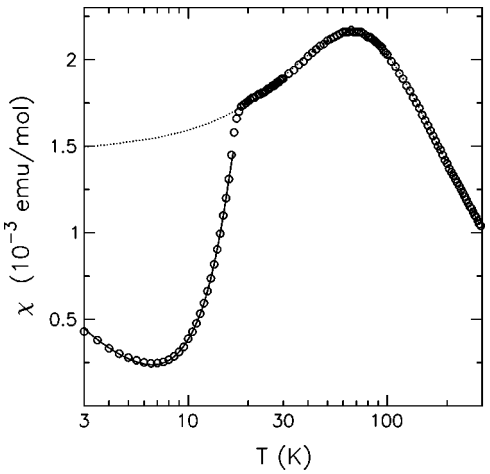

FIG. 2. Bulk magnetic susceptibility for $MEM(TCNQ)_2$. The dotted line represents a fit to a Bonner-Fisher expression at high temperature, which yields an exchange constant of 50.3 K. Note the knee at 18 K, indicative of a spin-Peierls transition. The low-temperature fit (solid line) is to a combination of Curie impurity and SP terms.

measurement of its bulk magnetic susceptibility χ using a Quantum Design MPMS superconducting quantum interference device (SQUID) magnetometer in Strasbourg (France). The data were taken in an applied magnetic field of 100 Oe and the result is shown in Fig. 2. The observed form of the susceptibility curve is in good agreement with results of Huizinga *et al.*[7] who find that the high-temperature dependence is well fit by a Bonner-Fisher[16] expression for a uniform Heisenberg antiferromagnet and that there is a sharp drop in the susceptibility at the SP transition, which is indicative of the opening of a gap in the magnetic excitation spectrum. Our determination of the susceptibility is more accurate than that in Ref. 7 where a Foner balance vibrating sample magnetometer was used.

The size of the gap at absolute zero, $\delta(0)$, can be estimated by using the result of Bulaevskii[17] who calculated the temperature dependence of χ in the dimerized state for varying degrees of dimerization in a Hartree-Fock approximation. We use the BCS-like dependence of the energy gap to determine the degree of dimerization at each temperature and then use the expression[7]

$$\chi(T)=\frac{Ng^2\mu_B^2}{k_B}\frac{\alpha(T)}{T}\exp\left(-\frac{2[1+d(T)]J\beta(T)}{T}\right), \tag{2.1}$$

where $\alpha(T)$ and $\beta(T)$ are tabulated in Bulaevskii's paper,[17] N is the number of spins per unit volume and $d(T)$ is the degree of dimerization, which is related to the BCS energy gap by

$$d(T)=\frac{\delta(T)}{2pJ}, \tag{2.2}$$

where $p\approx 1+2/\pi$.

We calculate the uniform exchange constant J by using the high-temperature Bonner-Fisher model and the best fit is found for $J=50.3(1)$ K, the experimental results being normalized to the theoretical prediction in this region. This is then used to fit the data in the SP state, where it is also necessary to include a term which takes account of defect spins which arise, for instance, from a chain with an odd number of spins. Spin freezing effects mean that the excess spin density due to a defect is spread further along the chain,[18,19] but we assume that the region of spin around a defect follows a simple Curie $1/T$ behavior (i.e., that the spin density is bound together as a single entity of spin 1/2). We shall return to a discussion of this later. The best fit is found for an impurity spin concentration of 0.357(2)% (assuming the impurities have spin 1/2) and $\delta(0)=21.3(1)$ K. The Bulaevskii result is scaled to the experimental results in the SP state by a factor of 0.7 (a similar factor is used by Huizinga *et al.*[7]).

μSR experiments[20] were carried out using the EMU and MuSR beamlines at the ISIS facility, Rutherford Appleton Laboratory (U.K.). In addition, some data were taken on the πM3 beamline at the Paul Scherrer Institute (Switzerland). In these experiments, a beam of almost completely spin polarized muons was implanted with a momentum of 30 MeV into the sample. The muons stop quickly (in $<10^{-9}$ s), without significant loss of polarization. The observed quantity is then the time evolution of the muon spin polarization, which can be detected by counting emitted decay positrons forward (f) and backward (b) of the initial muon spin direction; this is possibly due to the asymmetric nature of the muon decay, which takes place in a mean time of 2.2 μs.

We detected decay positrons by using scintillation counters placed around the sample. The numbers of positrons detected by forward (N_f) and backward (N_b) counters were recorded as a function of time and we then calculated the asymmetry function, $G_z(t)$:

$$G_z(t)=\frac{N_b(t)-\alpha_{cal}N_f(t)}{N_b(t)+\alpha_{cal}N_f(t)}, \tag{2.3}$$

where α_{cal} is an experimental calibration constant and differs from unity due to nonuniform detector efficiency. The quantity $G_z(t)$ is proportional to the average muon spin polarization, $P_z(t)$. The former quantity has a maximum value less than one since the positron decay is only preferentially, not wholly, in the direction of the muon spin. $P_z(t)$ has a maximum value of one (see Fig. 3 below), indicating polarization entirely in the beam direction.

Since the muon spin is expected to precess around any local magnetic fields of flux density B_i (with an angular frequency $\gamma_\mu B_i$, $\gamma_\mu/2\pi=135$ kHz/mT), we expect a distribution of internal fields to cause dephasing of the ensemble of muon spins and hence a relaxation in $G_z(t)$. Fluctuations in these fields affect the depolarization and so a consideration of the form of the asymmetry function, as well as its dependence on applied *external* magnetic fields, allows information to be obtained relating to the type of magnetic order and nature of spin fluctuations in materials.

We measured $MEM(TCNQ)_2$ in both zero field (ZF) and a range of applied longitudinal fields (LF) at temperatures ranging from 39 mK to 300 K, using a ^{4}He cryostat and an Oxford Instruments dilution refrigerator. Polycrystalline samples of $MEM(TCNQ)_2$ were packed in silver foil and mounted on a silver backing plate [silver is used since it

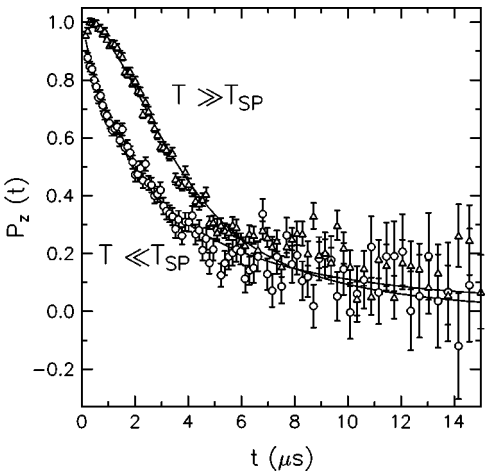

FIG. 3. Muon depolarization curves at temperatures well above and well below the SP transition. The fitted curve at the higher temperature comes from Eq. (3.3), whereas the low-temperature fit is to an expression formulated for an ensemble of slowly fluctuating dilute spins (Ref. 29).

gives a nonrelaxing muon signal and hence contributes only an additive constant to $G_z(t)$]. The asymmetry function may then be fitted using

$$G_z(t)=A_S P_z(t)+A_{Ag}, \tag{2.4}$$

where A_S and A_{Ag} represent the asymmetry contributions from muons stopping within the sample and silver backing plate, respectively. $P_z(t)$ then represents the polarization of muons stopping within the sample.

III. EXPERIMENTAL RESULTS

Two examples of muon depolarization curves, measured at temperatures either side of, but well away from, the SP transition, are shown in Fig. 3; there is a clear difference between the two. At high temperatures ($\gg T_{SP}$) the relaxation is Gaussian, whereas at low temperatures ($\ll T_{SP}$) it takes an approximately exponential form.

To explain this observation it is necessary to consider the nuclear and electronic spin systems which may cause the muon spin ensemble to relax. The nuclear spins are only a significant source of relaxation either when the electronic spins fluctuate too quickly for the muon spin to be affected (this is the so-called motional narrowing limit), or else are so dilute that their effect on the majority of muons is small. We are seeing relaxation due to nuclear spins at high temperatures: the electronic spins fluctuate rapidly leaving just the randomly orientated set of slowly moving nuclear spins to cause relaxation. The latter form a regular array of randomly orientated magnetic dipoles and in this case we expect a Gaussian field profile, which for a muon in a diamagnetic state in the static limit gives rise to the Kubo-Toyabe relaxation function,[21]

$$P_z^{st}(t,\Delta)=\frac{1}{3}+\frac{2}{3}(1-\Delta^2t^2)\exp\left(-\frac{1}{2}\Delta^2t^2\right), \tag{3.1}$$

where Δ/γ_μ is the width of the field distribution.

This expression is approximated well by a Gaussian at short times, but at longer times the polarization recovers to $\frac{1}{3}$ of its initial value. The lack of a long-time recovery in our measured data at high temperatures indicates a slow fluctuation of the spins. Assuming Markovian modulation of the flux density B_i at the muon site, with a rate ν,

$$\langle B_i(t)B_i(0)\rangle/\langle[B_i(0)]^2]\rangle=\exp(-\nu t), \tag{3.2}$$

we expect a depolarization function[22–24]

$$P_z^{dyn}(t,\Delta,\nu)=\exp(-\nu t)\Bigg(P_z^{st}(\Delta,t)+\nu\int_0^t P_z^{st}(\Delta,t_1)P_z^{st}\times(\Delta,t-t_1)dt_1+\nu^2\int_0^t\int_0^{t_2}P_z^{st}(\Delta,t_1)P_z^{st}\times(\Delta,t_2-t_1)dt_1dt_2+\cdots\Bigg). \tag{3.3}$$

The experimental data at 50 K (Fig. 3) are well fit using Eq. (3.3) with $\Delta=0.29$ MHz (which is typical of the small magnetic dipole moments associated with nuclear spins) and $\nu=0.45$ MHz (see Fig. 3). The relaxation is completely quenched in a small applied longitudinal field of 50 Oe, which is consistent with an almost static mechanism for depolarization. The application of a longitudinal field also confirmed the absence of any ''missing fraction'' of muon polarization, consistent with the presence of the muon in a diamagnetic state.

The change to exponential behavior happens at lower temperatures as the spin-Peierls gap widens. In general, exponential relaxation for diamagnetic muons can be caused by two alternative mechanisms. First, a periodic array of rapidly fluctuating electronic spins gives a relaxation of the form

$$P_z^{dyn}(\Delta,\nu)=\exp(-2\Delta^2t/\nu), \tag{3.4}$$

which is merely Eq. (3.3) in the fast fluctuating limit, $\nu/\Delta \gtrsim 5$, with Δ and ν now representing the field profile width and fluctuation rate of the electronic spins, respectively. Second, the presence of a dilute set of defect spins gives an approximately Lorentzian field distribution,[25,26] and will give rise to a Kubo-Toyabe function of the form[27]

$$P_z^{st,dil}(t,a)=\frac{1}{3}+\frac{2}{3}(1-at)\exp(-at), \tag{3.5}$$

where a/γ_μ is the Lorentzian field-profile width. This function also takes an exponential form at short times.

We ascribe the lowest temperature exponential behavior to a static mechanism for two reasons. First, the lowest temperature (39 mK) is much lower than any spin gap temperature, which is 21.3 K at $T=0$ (using the single-particle gap estimated from the susceptibility measurement). As electronic fluctuations are likely to be controlled by magnon excitations across this gap, we would expect any fast fluctuations to be effectively frozen out at 39 mK. Second, the field required to decouple the relaxation is consistent with a slowly fluctuating or static mechanism for depolarization. The low-temperature longitudinal field data closely follow the theoretical expression for a static Lorentzian distribution:[29]

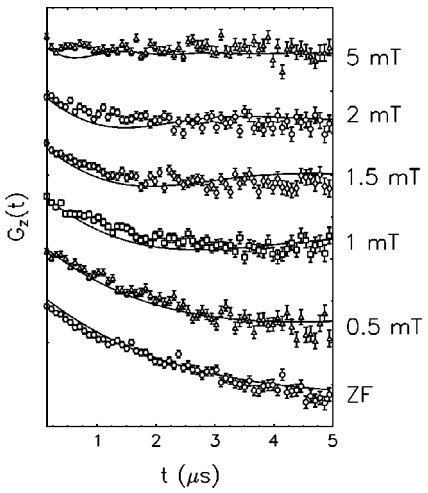

FIG. 4. Field dependence of the muon asymmetry function at 39 mK, fitted using Eq. (3.6). The curves are offset for clarity.

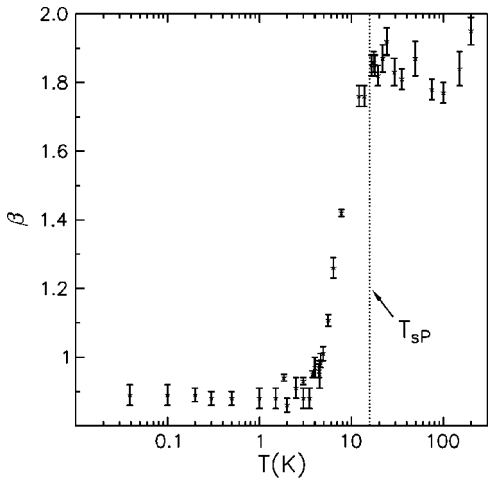

FIG. 5. Temperature dependence of the line-shape parameter (β) fitted using Eq. (3.7).

$$P_z^{dil,LF}(t,a,B_L)=1-\frac{a}{\gamma_\mu B_L}j_1(\gamma_\mu B_L t)\exp(-at)-\left(\frac{a}{\gamma_\mu B_L}\right)^2[j_0(\gamma_\mu B_L t)\exp(-at)-1]-\left[1+\left(\frac{a}{\gamma_\mu B_L}\right)^2\right]a\int_0^t j_0(\gamma_\mu B_L\tau)\times\exp(-a\tau)d\tau, \quad (3.6)$$

where j_0 and j_1 denote spherical Bessel functions and B_L is the flux density of the applied field. The fit to this function (over the first 5 μs of data where the effect of slow dynamics is comparatively small) is shown in Fig. 4 and uses only a single relaxation rate and measured applied field values, without further adjustment of parameters. Much higher fields would be required to decouple the muon from a rapidly fluctuating set of dense electron spins.

Before going on to discuss specific models for spin relaxation, we may follow the change in the depolarization mechanism by approximating the effect of two coexisting static field distributions to the phenomenological power Kubo-Toyabe function[28]

$$P_z^{total}(t,\lambda,\beta)=\frac{1}{3}+\frac{2}{3}[1-(\lambda t)^\beta]\exp\left(-\frac{(\lambda t)^\beta}{\beta}\right), \quad (3.7)$$

where λ is the relaxation rate and β is a parameter taking the value 1 for a purely Lorentzian static field distribution [Eq. (3.5)] and 2 for a Gaussian [Eq. (3.1)]. In the static regimes which we have discussed, any small fluctuations may be neglected if fitting is performed on only the first 5 μs of data, where their effect is small. We should thus be able to identify areas of certain different behaviors, which we will then go on to model separately.

The temperature dependence of β resulting from a fit to this expression is shown in Fig. 5. At high temperature the relaxation is Gaussian (nuclear relaxation) whereas the relaxation at low temperature is exponential (nuclear and electronic relaxation). The relaxation rate in these two regimes is similar; λ is approximately 0.25 MHz throughout. The temperature dependence of β shows that the change from one regime to the other happens over a temperature region which is of order 5 K in width and positioned at a temperature somewhat lower than the SP transition temperature, suggesting motional narrowing fluctuations do not slow down until the gap becomes quite large; we will return to this point later.

The results show that the low-temperature combination of an electronic Lorentzian and a nuclear Gaussian field profile have relaxation characterized by $\beta\sim 1$. This is in agreement with predictions of Monte-Carlo simulations by Crook and Cywinski,[28] where it is found that a Lorentzian profile of similar width to a coexistent Gaussian has a dominant effect in determining the shape of time-resolved spectra. For the purposes of the following discussion, we therefore assume that the only contribution to relaxation at the lowest temperatures is electronic in origin.

We may estimate the concentration of defects by adapting for the muon case an expression developed by Walstedt and Walker[26] which relates the relaxation of a nuclear spin to the number of surrounding defects, assuming a dipolar interaction between spins. Their expression assumes that the probability distribution of the magnetic field at a site with spherical coordinates r,θ with respect to the muon scales according to a well defined range function. In the case of spins pointing along the z axis, and interacting via the dipolar mechanism, this range function is proportional to $(1/r^3)(1-3\cos^2\theta)$. In order to get an idea of the field width due to defects, we assume that the muon is surrounded by electronic defect spins pointing along $\pm z$, and we obtain[26]

$$a=\frac{2\pi\mu_0\mu_B^2 g_\mu g_d S_d m_e n}{9\sqrt{3}m_\mu\hbar}, \quad (3.8)$$

where a is defined in Eq. (3.5), g_μ and g_d are the muon and defect g factors, S_d is the defect spin quantum number and n represents the concentration of defect spins. Using the low-temperature value of the relaxation rate, and assuming the defects have spin $\frac{1}{2}$ we obtain a concentration of defects of 6% of all spins. This estimate is interesting for two reasons. First, it is much larger than that estimated from magnetic

susceptibility, suggesting that we are not seeing intrinsic defects but that the muon itself may perturb its local environment to give the observed relaxation. Second, the calculated concentration is rather close to the dilute limit required for observation of the Lorentzian field distribution in metallic spin-glass systems, where the treatment is valid only for concentrations less than ~3–5 at. % (Ref. 29) [Eq. (3.8) can fail for higher concentrations as it assumes a relatively large minimum distance from test spin to defect]. We now therefore consider a specific simulation of a muon induced defect state in this organic material.

In organic compounds, one often finds a close bonding of muonium (a bound state of an electron and a muon) to regions rich in spin density on large molecules.[30] We have observed a low-field avoided level crossing resonance[31] in neutral TCNQ corresponding to an electron-muon hyperfine coupling of about 80 MHz.[32] This can be explained if muonium attaches to the central ring of the molecule where the electronic spin is delocalized. It is not unreasonable to assume such addition to the negatively charged TCNQ which exists in $MEM(TCNQ)_2$. However, above the SP temperature each TCNQ dimer has a single spin associated with it. The addition of muonium to this compound will cause this spin to pair up (with the muonium electron), thereby forming a singlet and leaving the muon in a diamagnetic environment. Below the SP transition, the basic unit is a spin-singlet tetramer and if we assume a similar close bonding of muonium to one of the two dimers we leave an unpaired spin on the other dimer in a higher energy level. We speculate that this spin may carry with it a local lattice distortion and can thus be regarded as a polaron. A static spin polaron will give rise to a Gaussian damping at short times. However, we would expect to have a distribution of distances to this defect since the muon will bind to a TCNQ dimer at different points, and the spin polaron may move to the next tetramer before localizing. We may thus have a distribution of distances and Gaussian widths, which for certain distributions can give Lorentzian-like behavior.

We assume that the spin position is uniformly distributed between two distances r_{min} and r_{max} from the muon site. Furthermore, each spin interacts with the muon via the dipolar spin Hamiltonian:

$$\mathcal{H}=D[\mathbf{S}\cdot\mathbf{I}-3(\mathbf{S}\cdot\mathbf{n})(\mathbf{I}\cdot\mathbf{n})]. \tag{3.9}$$

I is the muon spin, **S** is the electron spin, **n** is a unit vector in the direction which connects the two spins, and D is the dipolar coupling constant. We may calculate polycrystalline average muon polarization spectra by changing the angle between **n** and the z axis, and fit the result by varying r_{max} (we make the simplifying assumptions that D has the value for a point electron, which goes as $1/r^3$, and that r_{min} is fixed to the interdimer distance ~0.5 nm; note that the value of r_{min} has an effect mainly on the high-field distribution but that the width of the muon pulse at ISIS does not allow observation of higher frequencies).

The fit, which yields $r_{max}=2.37$ nm (or spin diffusion over a region up to 7 TCNQ molecules away on both sides of the muon site), is shown as the solid line in Fig. 6. The estimate from Eq. (3.8) had defects spaced by a mean distance of 2.27 nm (if we assume a cubic arrangement of defects), a number whose magnitude agrees well with our one-dimensional polaronic model despite the obvious differences between the two situations.

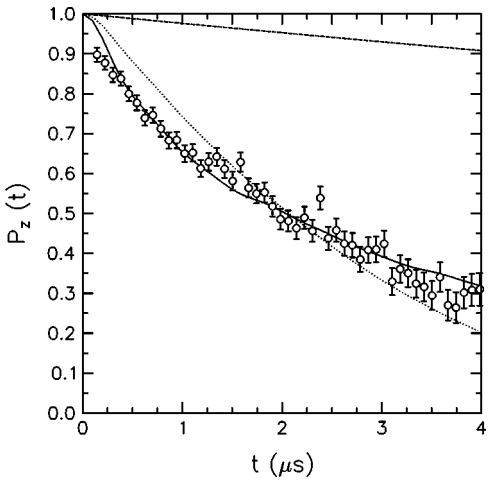

FIG. 6. Muon spin relaxation at 39 mK. Solid line: fitted curve resulting from a one-dimensional defect spin model; dotted line: fitted curve resulting from a three-dimensional distribution of defect spins; dashed line: relaxation curve due to spin-frozen regions around intrinsic defects.

The quality of the fit suggests that our simple model of uniform one-dimensional defect trapping provides at least a qualitative explanation of the true situation. We also tried a three-dimensional distribution of polarons, and the best fit for this model is shown in Fig. 6. The fit is clearly not as good, particularly at very short times where the difference between the two models is most evident and where inaccuracies due to any fluctuations will be smallest.

It has been suggested before that an intrinsic defect spin freezing mechanism causes relaxation in low dimensional spin-gap compounds at low temperatures.[33–35] Whilst this may hold true for inorganic materials, where muonium bonding to magnetic ions rarely occurs, we feel that the relaxation in $MEM(TCNQ)_2$ is more likely to be due to the perturbing effect of the muon described above. In order to determine how a spin-freezing mechanism would depolarize the muon spin, we have performed Monte Carlo simulations of the field distribution of a system of defect spins embedded in a spin-Peierls background around which spin-frozen regions develop.

Hansen *et al.*[18] performed quantum Monte Carlo simulations of the spin density in the vicinity of a spin-0 defect on a spin-Peierls chain. This situation would arise, for instance, in an odd numbered spin chain. They find that spin density is spread over some region along the chain, the length of which depends upon the stiffness of the lattice (in a stiffer lattice the effect of a defect will be felt over a larger region[18]). The spin density around the defect alternates with lattice site and there is both a staggered and uniform component to the local susceptibility. The total density integrates to $S_z=1/2$. We assumed in our simulations that the ratio of staggered to uniform components was 1/2 and that both components decay with a Gaussian dependence. These assumptions agree with Ref. 18, except that they find a small difference in the ratio for different Gaussian widths.

In our simulations, we calculated the field distribution by

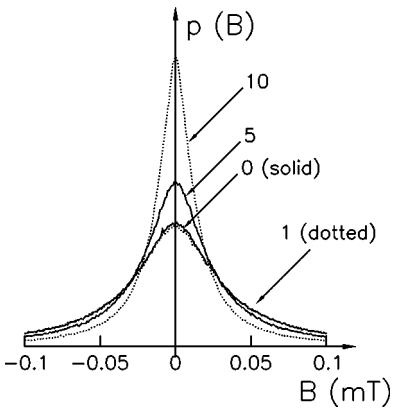

FIG. 7. Simulations of the spin-freezing effect. The numbers represent the Gaussian width of the spin-frozen region in number of lattice spacings.

assuming a random distribution of defect positions, which had a concentration given by our susceptibility estimate of 0.357%. We took a given position in the lattice and considered only the effect of the randomly generated nearest five spins to each site (an approximation which seems to be good when a comparison to simulations with more spins is considered). In each trial, the direction of spin chains for each surrounding spin-frozen region was assumed constant, but successive trials changed the direction of the chains according to an isotropic distribution. Furthermore, we assumed that spin density lies in a plane with orientation perpendicular to the chains, the azimuthal angle around the chain being a random variable. We also assume noninteracting spin-frozen regions.

The results of such a simulation, specific to the lattice parameters pertaining to $MEM(TCNQ)_2$ are shown in Fig. 7. The numbers on the figure represent the Gaussian width of the decay of the spin density; one can clearly see that there is a narrowing of the field distribution at longer decay lengths. This may be understood as follows. The spreading of the spin density over more lattice sites results in a smaller density *at each individual site*, an effect which would be expected to decrease the field distribution width. Added to this are the cancelling effects of having regions of alternating spin density. Despite the fact that a spreading of spin density means some spin density closer to the muon site, the other effects are clearly dominant in three dimensions.

The width of the Gaussian may be estimated using the result of Yoshioka and Suzumura,[19] who find, for the average lattice dimerization in a SP system with defects:

$$\frac{\langle u\rangle}{u_0}=1-2.347\left(\frac{J\pi}{2\delta^0}\right)c, \tag{3.10}$$

where u is the modulus of the (alternating) lattice displacement in the dimerized state, u_0 is the value of this parameter in the undoped state, c is the concentration of defects and δ^0 is the gap in the absence of defects, which is approximately unchanged from the gap in the presence of defects in the limit of low doping.[19]

In Ref. 18, it is found that in the vicinity of the defect the dimerization parameter is approximately sinusoidal, its (alternating) sign reversing as the defect region is traversed. Assuming such a sinusoidal dependence of the defect parameter, we obtain

$$\frac{\langle u\rangle}{u_0}=1-f\left(1-\frac{2}{\pi}\right). \tag{3.11}$$

f is the fraction of spins involved in the sinusoidal defect regions (this assumes widely spaced defect regions of equal length). Using Eqs. (3.10) and (3.11) we can obtain an estimate of the length of the defect region, and in $MEM(TCNQ)_2$ we find a region spanning 24 lattice spacings. Upon comparison of dimerization and local susceptibility data from Ref. 18, we find that this corresponds to a Gaussian standard deviation of around six lattice spacings. Such a spread *narrows* the distribution from the field width of 0.035 mT predicted from the simulation for zero spread, to a value of 0.021 mT. To explain the large relaxation in $MEM(TCNQ)_2$, we would have required a ten-fold increase in the field width. The simulated relaxation from the spin-freezing prediction is also shown in Fig. 6, where it can be seen that this model is wholly inadequate in describing the low-temperature data. Even if our original defect estimate from the magnetic susceptibility of $MEM(TCNQ)_2$ is somewhat in error due to our neglect of spin-freezing effects in that calculation, it seems unlikely that any revised estimate which takes this explicitly into account could explain the order of magnitude factor disagreement with the observed relaxation rate in this spin-Peierls system. (It should be noted that in a systematic study of the doped spin-Peierls system $Cu_{1-x}Zn_xGeO_3$,[36] nominal doping fractions were well reproduced by using a simple Curie term in the susceptibility.)

We now turn to the crossover between high- and low-temperature regimes (in the region 5–10 K, see Fig. 4) alluded to earlier. It seems likely that the change to exponential relaxation happens as the electronic fluctuations slow down when the SP gap opens in the magnetic excitation spectrum. We assume that these fluctuations are controlled by a second-order inelastic magnon scattering process in which a single electron may absorb a single quantum of energy from the system, causing it to undergo a spin flip (the first-order process is suppressed since the electron Zeeman energy is much lower than a typical magnetic excitation energy, which will be of order 21.3 K, the single-particle spin gap). An application[37] of the Fermi golden rule gives, for this second-order process,

$$\nu\propto\int_0^\infty n\left(\frac{E}{kT}\right)\left[n\left(\frac{E}{kT}\right)+1\right]M^2(E)\rho^2(E)dE, \tag{3.12}$$

where $M(E)$ is the matrix element for an electronic spin flip caused by inelastic scattering of an excitation of energy E, $\rho(E)$ is the density of magnon energy states, and n is the occupation number of the magnons which are assumed to follow Bose-Einstein statistics.

We now assume that the magnon dispersion has the form

$$E=Cq^2+\delta(T), \tag{3.13}$$

where $\delta(T)$ is the single-particle SP energy gap, q is the magnitude of the magnon wave vector and C is a stiffness

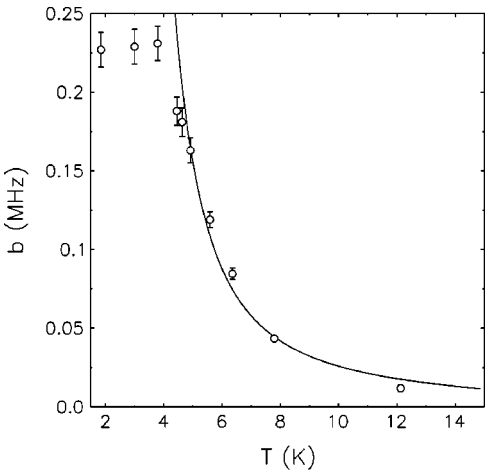

FIG. 8. Plot of b vs T, used to extract the energy gap [see Eq. (3.15)]. The fitted curve at higher temperature yields a BCS energy gap at $T=0$ of 17(1) K. At low temperatures, the relaxation saturates to a constant value which is determined by the (temperature-independent) defect spin concentration. In this region, Eq. (3.15) is not valid.

constant. This is a good approximation for low-energy, small q excitations[3] which are likely to be the most important for our low-temperature analysis.

Furthermore, we assume an energy-independent matrix element and then substitution of Eq. (3.13) into Eq. (3.12), including an approximately one-dimensional magnon density of states gives, in the limit of $\delta(T)/T \gg 1$,

$$\nu \propto \exp[-\delta(T)/T], \tag{3.14}$$

where $\delta(T)$ is the size of the BCS gap. This activated depedence is expected in the case of a spin gap.[35] Though the opening of the gap may cause many of the electron spins to collapse into singlets, the effect of the muon seems to be to locally liberate spin density and we assume that the nearby spin density causes a characteristic field profile of width Δ/γ_μ at the site. These depolarizing electrons act on the muon in the fast fluctuating limit [Eq. (3.4)] and the energy gap is BCS like. We fit the data using the product

$$P_z(b,t) = P_z^{nuc}(t)\exp(-bt), \tag{3.15}$$

of a static nuclear [P_z^{nuc}, fitted using Eq. (3.3) for the depolarization curves well above the crossover region and assumed to be temperature independent] and a fast fluctuating electronic component, characterized by $b = 2\Delta^2/\nu$. In Fig. 8 we show a plot of b against T and obtain an estimate of the energy gap by using Eq. (3.14). The best fit is shown and corresponds to $\delta(0) = 17(1)$ K, which is in good agreement with the 21.3 K estimate from the susceptibility data. A possible explanation for its slightly lower value may be our neglect of the temperature dependence of enhanced spin correlations in the tetramerized state on the static field width Δ which might be expected to cause a reduction in Δ at lower temperature.

A similar activated dependence of the nuclea-spin-relaxation rate, $1/T_1$ is seen in NMR experiments on another SP compound, $TTFCuS_4C_4$.[38,39] This was attributed to a similar mechanism of thermally activated excitations across the magnetic gap. The different time window of the technique (compared to μSR) means that this is observed as a decrease in the spin-lattice relaxation rate at lower temperature.

The turnover of the muon relaxation in $MEM(TCNQ)_2$ at lower temperature (Fig. 8) happens once the spins slow down and the relaxation rate saturates to a constant value which is determined only by the temperature-independent distribution of muon induced defects. In this limit, Eq. (3.15) is no longer valid and the fits it produces are poor. The reader is referred to the earlier discussion of the lowest temperature relaxation.

IV. CONCLUSIONS

In this study, we have demonstrated the usefulness of the muon technique as both a detector of spin dynamics associated with the opening of an energy gap in the magnon excitation spectrum, and as a probe of the low-temperature activity of defects which do not follow the nonmagnetic behavior of the majority of spins.

The results of this study are in broad agreement with the previous muon studies of spin-Peierls compounds of Lappas *et al.*[40] and Garçia-Muñoz *et al.*[41] who studied $CuGeO_3$. A similar slowing down in spin fluctuations is observed below T_{SP}, though it was not directly related to the opening of an energy gap in the magnetic excitation spectrum. Also, the significance of a low-temperature defect contribution was not pointed out, though this would be required to explain the large drop in Gaussian relaxation rate observed in $CuGeO_3$ at low temperatures (this point is made by Tchernyshyov *et al.*[42] in a similar study).

In the case of materials with a nonmagnetic singlet ground state, the importance of dilute spin defects is enhanced once the magnetic gap opens at low temperatures.[43] However, we have demonstrated that this does not preclude the use of the muon as a detector of changes in spin dynamics associated with the formation of an energy gap in this material. In an inorganic material which has a temperature-independent spin gap a similar crossover between dynamics-dominated and defect-dominated behavior has also been observed.[44] This suggests that this phenomenon may be quite general in materials which show spin gaps. We have also demonstrated that the muon cannot be regarded merely as a passive probe in this organic system. The muon spin itself seems to play a major role in locally creating a spin defect by breaking a singlet pair. This could give rise to the relaxation which we have ascribed to stationary polaronic states and which is only revealed when the other sources of relaxation have frozen out.

ACKNOWLEDGMENTS

We are grateful to R. Cywinski, Y. J. Uemura, and J. H. Brewer for useful discussions and to R. Poinsot (Strasbourg), P. J. C. King (RAL) and U. Zimmerman (PSI) for valuable technical assistance. This work was supported by the EPSRC (UK), the CNRS (France), the Japanese Ministry of Education and the European Science Foundation. T.J. would like to thank the European Commission for financial support in the framework of the TMR program.

*Electronic address: b.lovett1@physics.ox.ac.uk
†Also at RIKEN-RAL, Rutherford Appleton Laboratory, Chilton, Didcot OX11 0QX, U.K.

[1] G. Beni and P. Pincus, J. Chem. Phys. **57**, 3531 (1972).
[2] J. W. Bray, H. R. Hart, Jr., L. V. Interrante, L. S. Jacobs, J. S. Kasper, G. D. Watkins, and S. H. Wee, Phys. Rev. Lett. **35**, 744 (1973).
[3] J. W. Bray, L. V. Interrante, I. S. Jacobs, and J. C. Bonner, *Extended Linear Chain Compounds* (Plenum, New York, 1983), Vol. 3, pp. 353-415.
[4] E. Pytte, Phys. Rev. B **10**, 4637 (1974).
[5] S. J. Blundell, F. L. Pratt, P. A. Pattenden, M. Kurmoo, K. H. Chow, S. Tagaki, Th. Jestädt, and W. Hayes, J. Phys.: Condens. Matter **9**, L119 (1997).
[6] R. E. Peierls, *Quantum Theory of Solids* (Oxford University Press, London, 1955).
[7] S. Huizinga, J. Kommandeur, G. A. Sawatzky, B. T. Thole, K. Kopinga, W. M. J. de Jonge, and J. Roos, Phys. Rev. B **19**, 4723 (1979).
[8] R. J. J. Visser, S. Oostra, C. Vettier, and J. Voiron, Phys. Rev. B **28**, 2074 (1983).
[9] B. van Bodegom, B. C. Larson, and H. A. Mook, Phys. Rev. B **24**, 1520 (1981).
[10] G. Li, L. S. Lee, V. C. Long, J. L. Musfeldt, Y. J. Wang, M. Almeida, A. Revcolevski, and G. Dhalenne, Chem. Mater. **10**, 1115 (1998).
[11] Y. Tanaka, N. Satoh, and K. Nagasaka, J. Phys. Soc. Jpn. **59**, 319 (1990).
[12] H. Norija, T. Hamamoto, O. Fujita, J. Akimitsu, S. Tagaki, and M. Motokawa, J. Magn. Magn. Mater. **177**, 687 (1998).
[13] Y. Matsuda, T. Sakakibara, T. Goto, and Y. Ito, J. Phys. Soc. Jpn. **55**, 3225 (1986).
[14] P. I. Kuindersma, G. A. Sawatzky, J. Kommandeur, and C. J. Schinkel, J. Phys. C **8**, 3016 (1975).
[15] M. C. Cross and D. S. Fisher, Phys. Rev. B **19**, 402 (1979).
[16] J. C. Bonner and M. E. Fisher, Phys. Rev. A **135**, A640 (1964).
[17] L. N. Bulaevskii, Fiz. Tverd. Tela (Leningrad) **11**, 1132 (1969) [Sov. Phys. Solid State **11**, 921 (1969)].
[18] P. Hansen, D. Augier, J. Riera, and D. Poilblanc, Phys. Rev. B **59**, 13 557 (1999).
[19] H. Yoshioka and Y. Suzumura, J. Phys. Soc. Jpn. **66**, 3962 (1997).
[20] J. H. Brewer, *Encyclopedia of Applied Physics* (VCH Publishers, New York, 1994), Vol. 11, pp. 23-53; A. Schenck, *Muon Spin Rotation: Principles and Applications in Solid State Physics* (Hilger, London, 1985); S. F. J. Cox, J. Phys. C **20**, 3187 (1987); A. Schenck and F. N. Gygax, *Handbook of Magnetic Materials* (North-Holland, Amsterdam, 1995), Vol. 9, pp. 57–302; P. Dalmas de Réotier and A. Yaouanc, J. Phys.: Condens. Matter **9**, 9113 (1997).
[21] R. Kubo and T. Toyabe, *Magnetic Resonance and Relaxation* (North-Holland, Amsterdam, 1967), p. 810.
[22] Y. J. Uemura, Hyperfine Interact. **8**, 739 (1981).
[23] Y. J. Uemura, R. S. Hayano, J. Imazato, N. Nishida, and T. Yamazaki, Solid State Commun. **31**, 731 (1979).
[24] R. S. Hayano, Y. J. Uemura, J. Imazato, N. Nishida, T. Yamazaki, and R. Kubo, Phys. Rev. B **20**, 850 (1979).
[25] C. Held and M. W. Klein, Phys. Rev. Lett. **35**, 1783 (1975).
[26] R. E. Walstedt and L. R. Walker, Phys. Rev. B **9**, 4857 (1974).
[27] R. Kubo, Hyperfine Interact. **8**, 731 (1981).
[28] M. R. Crook and R. Cywinski, J. Phys.: Condens. Matter **9**, 1149 (1997).
[29] Y. J. Uemura, T. Yamazaki, D. R. Harshman, M. Senba, and E. J. Ansaldo, Phys. Rev. B **31**, 546 (1985).
[30] S. J. Blundell, Appl. Magn. Reson. **13**, 155 (1997).
[31] M. Heming, E. Roduner, B. D. Patterson, W. Odermatt, J. Schneider, H. Baumeler, H. Keller, and I. M. Savić, Chem. Phys. Lett. **128**, 100 (1986); R. F. Kiefl, Hyperfine Interact. **32**, 707 (1986).
[32] F. L. Pratt, S. J. Blundell, Th. Jestädt, B. W. Lovett, R. M. Macrae, and W. Hayes (unpublished).
[33] G. M. Luke, Y. Fudamoto, M. J. P. Gingras, K. M. Kojima, M. Larkin, J. Merrin, B. Nachumi, and Y. J. Uemura, J. Magn. Magn. Mater. **177**, 754 (1998).
[34] K. M. Kojima, Y. Fudamoto, M. Larkin, G. M. Luke, J. Merrin, B. Nachumi, Y. J. Uemura, M. Hase, Y. Sasago, K. Uchinokura, Y. Ajiro, A. Revcolevschi, and J.-P. Renard, Phys. Rev. Lett. **79**, 503 (1997).
[35] Y. Fudamoto, K. M. Kojima, M. I. Larkin, G. M. Luke, J. Merrin, B. Nachumi, Y. J. Uemura, M. Isobe, and Y. Ueda, Phys. Rev. Lett. **83**, 3301 (1999).
[36] K. Manabe, H. Ishimoto, N. Koide, Y. Sasago, and K. Uchinokura, Phys. Rev. B **58**, R575 (1998).
[37] S. R. Dunsiger, R. F. Keifl, K. H. Chow, B. D. Gaulin, M. J. P. Gingras, J. E. Greedan, A. Keren, K. Kojima, G. M. Luke, W. A. MacFarlane, N. P. Raju, J. E. Sonier, Y. J. Uemura, and W. D. Wu, Phys. Rev. B **54**, 9019 (1996); S. R. Dunsiger, R. F. Keifl, K. H. Chow, B. D. Gaulin, M. J. P. Gingras, J. E. Greedan, A. Keren, K. Kojima, G. M. Luke, W. A. MacFarlane, N. P. Raju, J. E. Sonier, Y. J. Uemura, and W. D. Wu, J. Appl. Phys. **79**, 6636 (1996).
[38] L. S. Smith, E. Ehrenfreund, A. J. Heeger, L. V. Interrante, J. W. Bray, H. R. Hart, Jr., and L. S. Jacobs, Solid State Commun. **19**, 377 (1976).
[39] E. Ehrenfreund and L. S. Smith, Phys. Rev. B **16**, 1870 (1977).
[40] A. Lappas, K. Prassides, A. Amato, R. Feyerherm, F. N. Gygax, and A. Schenk, Z. Phys. B: Condens. Matter **96**, 223 (1994).
[41] J. L. Garçia-Muñoz, M. Suaadi, and B. Martínez, Phys. Rev. B **52**, 4288 (1995).
[42] O. Tchernyshyov, A. S. Blaer, A. Keren, K. Kojima, G. M. Luke, W. D. Wu, Y. J. Uemura, M. Hase, K. Uchinokura, Y. Ajiro, T. Asano, and M. Mekata, J. Magn. Magn. Mater. **140-144**, 1687 (1995).
[43] K. M. Kojima, Appl. Magn. Reson. **13**, 111 (1997).
[44] Th. Jestädt, R. I. Bewley, S. J. Blundell, W. Hayes, B. W. Lovett, F. L. Pratt, and R. C. C. Ward, J. Phys.: Condens. Matter **10**, L259 (1998).